HHS Public Access

Author manuscript

J Mol Med (Berl). Author manuscript; available in PMC 2016 January 06.

Published in final edited form as:

J Mol Med (Berl). 2015 August ; 93(8): 845–856. doi:10.1007/s00109-015-1311-1.

Deletion of *Panx3* Prevents the Development of Surgically Induced Osteoarthritis

Paxton M. Moon[1], **Silvia Penuela**[2], **Kevin Barr**[2], **Sami Khan**[1], **Christopher L. Pin**[1,3,4,5], **Ian Welch**[6], **Mukundan Attur**[7], **Steven B. Abramson**[7], **Dale W. Laird**[1,2], and **Frank Beier**[1,5]

Dale W. Laird: Dale.Laird@schulich.uwo.ca; Frank Beier: fbeier@uwo.ca

[1]Departments of Physiology and Pharmacology, University of Western Ontario, London, Ontario, Canada

[2]Anatomy and Cell Biology, University of Western Ontario, London, Ontario, Canada

[3]Paediatrics, University of Western Ontario, London, Ontario, Canada

[4]Oncology, University of Western Ontario, London, Ontario, Canada

[5]Children's Health Research Institute, London, Ontario, Canada

[6]Department of Animal Care Services, University of British Columbia, Vancouver, British Columbia, Canada

[7]Division of Rheumatology, NYU Hospital for Joint Diseases, New York University School of Medicine and NYU Langone Medical Cente, New York, NY, USA

Abstract

Osteoarthritis (OA) is a highly prevalent, disabling joint disease with no existing therapies to slow or halt its progression. Cartilage degeneration hallmarks OA pathogenesis, and pannexin 3 (Panx3), a member of a novel family of channel proteins, is upregulated during this process. The function of Panx3 remains poorly understood, but we consistently observed a strong increase in Panx3 immunostaining in OA lesions in both mice and humans. Here, we developed and characterized the first global and conditional *Panx3* knockout mice to investigate the role of Panx3 in OA. Interestingly, global *Panx3* deletion produced no overt phenotype and had no obvious effect on early skeletal development. Mice lacking *Panx3* specifically in the cartilage and global *Panx3* knockout mice were markedly resistant to the development of OA following destabilization of medial meniscus surgery. These data indicate a specific catabolic role of Panx3 in articular cartilage and identify Panx3 as a potential therapeutic target for OA. Lastly, while Panx1 has been linked to over a dozen human pathologies, this is the first *in vivo* evidence for a role of Panx3 in disease.

Correspondence to: Dale W. Laird, `Dale.Laird@schulich.uwo.ca`; Frank Beier, `fbeier@uwo.ca`.

Paxton M. Moon and Silvia Penuela contributed equally to this work.

Electronic supplementary material The online version of this article (doi:10.1007/s00109-015-1311-1) contains supplementary material, which is available to authorized users.

Conflict of Interest The authors declare that they have no competing interest.

Keywords

DMM; Cartilage; Mice; Pannexin 3; Osteoarthritis

Introduction

Osteoarthritis (OA) is one of the most disabling conditions worldwide, affecting an estimated 250 million people [1]. OA is associated with excess morbidity and mortality in affected patients and is, therefore, responsible for a tremendous socioeconomic burden [2–4]. Our ability to effectively treat this disease is hampered by a limited understanding of the molecular mechanisms that cause it, resulting in a lack of therapeutic strategies to modify progressive joint damage characteristic of OA. Current practices for OA treatment are limited to symptomatic management [5]. The end stage approach to unmanageable OA is joint replacement surgery, which is not a permanent solution, highlighting a need for more effective alternatives [6].

OA is hallmarked by a gradual destruction of the articular cartilage, but involves pathological changes in all joint tissues. Common features include subchondral sclerosis, synovial inflammation/hyperplasia, and osteophyte formation, which together cause severe pain leading to loss of joint function [7]. The onset of cartilage degeneration is triggered by an imbalance between anabolic and catabolic processes, resulting in gradual joint destruction [8]. Several factors, including small molecules like ATP and pro-inflammatory cytokines such as interleukin 1 beta (IL-1β), have been shown to activate catabolic processes in chondrocytes [9]. However, the factors stimulating their production and release in chondrocytes during the early stages of OA remain poorly understood. A previous study in our lab used microarray analysis of cartilage obtained in the early stages of surgically induced OA in rats to identify such mechanisms [10]. *Panx3*, a gene also upregulated in the prehypertrophic and hypertrophic zone of the murine growth plate, was observed to be increased fourfold in OA cartilage compared to controls [10, 11].

Panx3 encodes the protein pannexin 3 (Panx3), which, like the other two pannexin family members (Panx1 and Panx2), is a channel forming glycoprotein [12]. The pannexins were discovered in 2000 by Panchin and colleagues [13] and have since been implicated in a diverse array of normal and pathophysiological processes [14–16]. In chondrocytes, in vitro studies demonstrated that Panx3-mediated ATP release accelerated hypertrophic differentiation, a process critical for skeletal development [17]. Normally restricted to the transient cartilage of the growth plate, this catabolic process is recapitulated in OA and is likely an important factor stimulating cartilage breakdown [18, 19]. Chondrocyte hypertrophy drives cartilage resorption in preparation for bone deposition and is, therefore, paired with increased catabolic enzyme expression, most notably MMP13 [20]. Additionally, *Panx3* is a target of the master hypertrophic regulator RUNX2, a transcription factor that also drives increased MMP13 expression [21]. Combined, this evidence suggests a role for Panx3 in driving ectopic chondrocyte hypertrophy in OA. Thus, we hypothesized that loss of Panx3 will delay the onset or progression of this disease.

In this study, we examined Panx3 expression and localization in both murine and human OA and explored the *in vivo* role of *Panx3* by creating the first *Panx3* knockout mice. We used these novel mouse lines to investigate the effects of global (*Panx3*$^{-/-}$) and cartilage-specific (*Panx3*$^{fl/fl}$:*Col2cre*) *Panx3* deletion on skeletal development and osteoarthritis.

Materials and Methods

Generation of Panx3 Knockout Mice

The *Panx3*$^{fl/fl}$ strain used in this study was generated from an embryonic cell line (JM8A3.N1 Agouti (A/a), C57BL/6N), obtained from the NCRR-NIH supported KOMP Repository (www.komp.org) and generated by the Wellcome Trust Sanger Institute and the Mouse Biology Program (www.mousebiology.org) at the University of California Davis. Clone EPD0670_4_C10 for allele Panx3tm1a (KOMP)Wtsi of targeting project CSD24494, was engineered as a “Knockout First” (promoter driven) cassette using targeting vector PG00057_Y_A09_2.

Panx3$^{fl/fl}$ mice were generated through blastocyst injection into a C57BL/6N pseudo-pregnant female by the London Regional Transgenic and Gene Targeting Facility at the University of Western Ontario. Chimeric founders were mated with C57BL/6N mice and offspring showing germline transmission of the targeting allele were mated to C57BL/6J FLP deleter mice (B6(C3)-Tg(Pgk1-FLPo)10Sykr/J; Jaxmice #011065 (Jackson Laboratories, Bar Harbour, ME, USA) for removal of the FRT flanked selection cassette. Litters of the floxed Panx3 (*Panx3fl/fl*) mice were first crossed with C57BL/6J Cre deleter mice (B6.C-Tg(CMV-cre)1Cgn/J; Jaxmice # 006054) for germline deletion of the targeted exon. Offspring mice were PCR genotyped to confirm the hemizygous deletion of *Panx3* exon 2. Mice hemizygous for the deleted exon were further crossed to produce homozygous null mice. Mating *Panx3*$^{fl/fl}$ mice with CMV-*cre* mice generated global *Panx3*$^{-/-}$ mice. *Cre* recombinase was out-bred following the generation of the *Panx3*$^{-/-}$ line. Chondrocyte specific *Panx3*-deficient mice were generated through mating *Panx3*$^{fl/fl}$ mice with C57BL/6J *Col2a1-Cre* mice [22–25].

Validation of Panx3 Ablation

PCR genotyping was performed to verify the lack of a *Panx3* exon2 amplicon in *Panx3* null mice (*Panx3*$^{-/-}$) using an upper primer annealing to the intron just upstream of exon 2 in the floxed allele and the lower primer annealing to an exon 2 sequence. RT-PCR was performed on total RNA from mouse cartilage (extracted with a RNeasy kit; QIAGEN, Venlo, Limburg, Netherlands), with primers designed to amplify a product bridging the intron between exons 3 and 4 of Panx3, to verify that these exons are also not transcribed in the null mice. Western blots of protein lysates from 3-week-old wild type and null mice cartilage (from outer ears or tail tips) were performed as described earlier [26, 27] and probed with the anti-Panx3 antibody (CT-379), also previously described [27]. β-tubulin was used as loading control.

Animals and Surgery

All animal experiments were approved by the Animal Use Subcommittee at the University of Western Ontario and conducted in accordance with guidelines from the Canadian Council on Animal Care. Experimental OA was induced at 20 weeks of age by performing DMM surgery on the left hind limb of male *Panx3*$^{fl/fl}$ (control) or *Panx3*$^{fl/fl}$:*Col2cre*$^{+/-}$ mice as described [28–30]. Sham-operated animals were used as controls. 18 total mice were used for the surgical trial, nine *Panx3*$^{fl/fl}$ (control; 5 DMM and 4 Sham) and nine *Panx3*$^{fl/fl}$:-*Col2cre* (5 DMM and 4 Sham). Littermates were used within each treatment group (DMM or Sham) to control for any variability associated with differing genetic backgrounds. All mice were sacrificed 8 weeks post-surgery by CO^2 asphyxiation, and both operated and unoperated (right) limbs were harvested. The same protocol was used to assess OA progression following DMM surgery in control (WT) and globally deficient *Panx3*$^{-/-}$ mice (*N*=3).

Analysis of Skeletal Development

Newborn (P0) and 21 day old (P21) *Panx3*$^{-/-}$ and control mice were sacrificed using intraperitoneal Euthanyl (pentobarbital) injections (Animal Health Inc. Cambridge, ON, Canada). Alcian Blue/Alizarin Red was used to stain whole skeletons of 21-day-old mice as described [22, 23] (Sigma, St. Louis, MO, USA). Long bones (tibia, femur, and humerus) were isolated at P0 and P21, fixed in 4 % paraformaldehyde (PFA), decalcified in ethylenediaminetetraacetic acid (EDTA; Bioshop, Burlington, ON, Canada), and embedded in paraffin wax. Safranin-O/Fast Green was used to stain paraffin sections cut down the length of the long bones. Additionally, P0 tibia and femur growth plates and P21 tibia, humerus, and femur lengths were measured. Three wild-type and 3 *Panx3* null mice from each time point (P0 or P21) were used for each trial described above.

Histopathology of the Knee

Knees harvested 8 weeks following surgeries were fixed in 4 % PFA (Sigma), decalcified in EDTA, and embedded in paraffin wax. Frontal sections were cut by the Molecular Pathology Facility and stained with Safranin-O/Fast Green (Sigma/VWR, Radnor, PA, USA) as previously described [31]. Ten sections through the entire joint were scored according to the OARSI histopathology scoring system by three blinded observers [32]. Scores from 0 to 6 were assigned to the medial and lateral tibia plateaus and femoral condyles based on depth and width of lesion. A score of 0 corresponds to healthy cartilage and is what is commonly seen in the joints of sham-operated animals. Scores ranging from 0.5 to 6 reflect increasing severity of cartilage degeneration. Focal aggrecan loss, surface fibrillations, and cracks without cartilage loss are assigned scores of 0.5, 1, or 2, respectively. Varying degrees of cartilage erosion ranging from less than 25 % to greater than 75 % are represented by scores from 3 to 6. Individual scores are averaged across observers and summed for each sample. These are then used to determine quadrant, compartment, and whole joint scores. These scores are than compared between *Panx3*$^{fl/fl}$ and *Panx3*$^{fl/fl}$:*Col2-cre*$^{+/-}$ mice (*N*=5/4 (DMM/sham)) or WT and *Panx3*$^{-/-}$ mice (*N*=3).

Immunohistochemistry

Frontal sections of paraffin embedded knees and long bones were used for immunohistochemical analysis. Sections were dewaxed and re-hydrated as previously described [25, 31, 30]. Custom-made site-directed anti-Panx1 (CT-395) and anti-Panx3 (CT-379) antibodies (reported earlier by [27]) targeting mouse pannexin sequences and commercial anti-MMP13 (Protein Tech, Chicago, IL, USA) and anti-Collagen II (Fitzgerald, Acton, MA, USA) primary antibodies were used for immunolabeling. HRP-conjugated goat anti-rabbit secondary antibodies (Biorad, Hercules, CA, USA) were used with diaminobenzidine substrate (Sigma) to reveal immunopositive staining. Methyl Green (Sigma) was used to counterstain sections.

Human Cartilage

Knee OA cartilage samples were obtained from two patients diagnosed with advanced OA (patients were both female, 60 and 62 years of age) and undergoing knee replacement surgery under the guidelines of the Institutional Review Board of New York University (NYU) School of Medicine protocol #H9018 for use of surgically discarded human tissues. Regions of the tibial plateau and femoral condyle showing signs of cartilage degeneration along with regions showing no macroscopic signs of damage as internal controls was extracted from two female patients aged 60 and 62. Tissues were decalcified for 48 h in Formical (Decal Chemical Corp, Lodi, CA, USA) and subsequently embedded in Paraffin wax. Sections of tissue were stained with Safranin-O/Fast green, to assess proteoglycan content and immunostained with anti-Panx3 (CT379) antibody. Representative sections from lesion and non-lesion control tissue are presented; N=2.

Measurement of Osteophyte Size

To determine the area of osteophytes observed in DMM-operated control animals, three sections at similar depths spanning the medial anterior compartment of the joint were selected from each animal and imaged at ×200 magnification. Using the Leica Application Suite software, the margins of the osteophyte were traced and the area was determined using the software represented in square microns (mm^2).

Statistical Analysis

For comparisons of bone lengths, growth plates and OARSI scores between control and *Panx3*$^{-/-}$ DMM-operated animals, two-tailed student *t* tests were employed. Two-way analysis of variance (ANOVA) was used to compare all four groups from cartilage specific *Panx3* deficient *in vivo* surgical trial with Bonferroni post hoc analysis. All statistical analyses were performed using GraphPad Prism (Graphpad Software Inc. La Jolla, CA, USA) v.6.0. $N \geq 3$ for all animal experiments.

Results

Generation of *Panx3*$^{fl/fl}$ mice for global Panx3 ablation

Using *Panx3*-targeted embryonic cells (ES) with a C57BL/6N origin from the Knockout Mouse Project repository (Fig. 1a), we generated a genetically-modified mouse line using

the *Cre/loxP* recombinase system for constitutive and tissue-specific deletion of *Panx3*. We first generated ubiquitous KO mice by breeding $Panx3^{fl/fl}$ mice to a CMV-Cre driver strain [33]. Homozygous null mice were identified by PCR genotyping (Fig. 1b) and later confirmed by RT-PCR (Fig. 1c) and Western blotting (Fig. 1d) to lack Panx3 expression in tissues rich in cartilage or bone, such as the outer ear and the tail, where Panx3 is abundant in the wild type control. $Panx3^{-/-}$ mice were found to be viable and fertile. However, litter sizes of $Panx3^{+/-} \times Panx3^{+/-}$ crosses as well as $Panx3^{-/-} \times Panx3^{-/-}$ crosses were significantly smaller than those of $Panx3^{+/+} \times Panx3^{+/+}$controls (Fig. 1e). Furthermore, $Panx3^{+/-} \times Panx3^{+/-}$ crosses failed to generate the predicted number of $Panx3^{-/-}$ offspring based on a normal Mendelian ratio (~25 %), and instead, produced only 8 % of $Panx3^{-/-}$ pups (Fig. 1f). Body weights of viable $Panx3^{-/-}$ males at 12 weeks of age did not show any significant differences compared to wild-type controls (Fig. 1G), and the overall appearance of 4-week-old and 8-month-old $Panx3^{-/-}$ mice was similar to the controls with no overt phenotypes (Fig. 1h, i).

Global Loss of Panx3 Has no Major Effect on Skeletal Development

Current evidence shows that Panx3 is an important regulator of hypertrophic differentiation of chondrocytes [17]. Due to the importance of this process during skeletal development, we investigated the effects of global Panx3 loss on skeletal development. Growth plates of $Panx3^{-/-}$ mice were compared to wild-type (WT) C57BL/6 mice at P0 and P21. There were no major abnormalities in growth plate morphology and organization in $Panx3^{-/-}$ mice compared to WT (Fig. 2a). This is complemented by the absence of differences in the length of the growth plate and its individual zones (Fig. 2b, c). At P0 and P21, Panx3 immunostaining appears concentrated in the pre-hypertrophic zone in WT mice, but this staining is absent in *Panx3* null growth plates, confirming its deletion (Fig. 2a). Whole skeletal preparations of P21 WT and $Panx3^{-/-}$ mice stained with Alizarin Red and Alcian Blue revealed no gross skeletal abnormalities in $Panx3^{-/-}$ mice (Fig. 2d). Measurements of humerus, femur, and tibia lengths confirmed that there were no differences in size between WT and $Panx3^{-/-}$ mice at this stage (Fig. 2d). Skeletal morphology (data not shown) and long bone lengths (Fig. 2d) remain similar between WT and null mice at 6 weeks of age.

Panx3 and MMP13 Immunostaining is Increased in Areas of Cartilage Degeneration in Mice and Humans

Immunostaining for Panx3 and MMP13 was done on paraffin sections obtained from 12-week-old male WT C57BL/6 mice that either underwent destabilization of medial meniscus (DMM) surgery to induce OA [28, 29] or sham surgery. At 5 weeks post-surgery, mice displayed mild OA. Histologically, this appeared as loss of proteoglycan staining in Safranin-O/Fast Green staining and as delamination of superficial cartilage from the underlying calcified matrix (Fig. 3a). Strong Panx3 staining was localized in areas of mild cartilage degeneration. Similarly, immunostaining for MMP13 on serial sections of lesions revealed strong staining in the same areas of cartilage degeneration. Cartilage from sham-operated animals appeared healthy and did not stain strongly for either Panx3 or MMP13 (Fig. 3a).

In addition to being localized to cartilage lesions in murine OA, Panx3 was also detected in human osteoarthritic cartilage (Fig. 3b). Tissue was obtained from both lesioned and non-weight-bearing (control) regions of the knee from patients undergoing joint replacement surgeries. In areas showing histological features of OA such as decreased proteoglycan staining, chondrocyte clustering, and cartilage surface degeneration, we observed an increased in Panx3 immunostaining compared to control regions.

Cartilage-Specific Deletion of Panx3 Protects Against Osteoarthritis Development In Vivo

To assess the importance of Panx3 in OA in vivo, we generated cartilage-specific *Panx3* KO mice to specifically address its role in chondrocytes in a model of post-traumatic OA. In agreement with the data from *Panx3*$^{-/-}$ mice, these mice did not show any defects in skeletal development and growth (data not shown). We performed DMM surgery to induce OA in a 20-week-old control (*Panx3*$^{fl/fl}$) and *Panx3*$^{fl/fl}$:-*Col2cre* mice that are deficient in *Panx3* specifically in chondrocytes. Paraffin sections of knees isolated 8 weeks post-surgery were stained with Safranin-O/Fast Green and scored according to the OARSI histopathology scoring system [32]. Control mice developed cartilage degeneration as expected. Histologically, advanced cartilage degeneration and osteophyte formation was seen in DMM-operated control but not in *Panx3*$^{fl/fl}$:*Col2-cre* mice, which showed at worst minor proteoglycan loss (Fig. 4a, b). Whole joint scores confirmed significantly reduced OA severity in *Panx3*$^{fl/fl}$:*Col2-cre* (Fig. 4e). The medial compartment is most severely affected in DMM surgery and scores from medial tibia plateaus and medial femoral condyles are significantly lower in *Panx3*$^{fl/fl}$:-*Col2-cre* mice (Fig. 4a). Medial compartment (Fig. 4c, d) and whole joint scores (Fig. 4e) from sham-operated mice of either genotype revealed no damage. This was complemented by the absence of histological signs of cartilage degeneration in Safranin-O/Fast Green stained sections (Fig. 4a, b).

Type II Collagen Staining is Decreased, While MMP13 Staining is Increased in DMM-Operated *Panx3*$^{f/f}$ Mice

Type II collagen is a critical matrix molecule in articular cartilage and its destruction marks the onset of terminal OA. As expected, matrix and pericellular type II collagen staining appears reduced in DMM-operated *Panx3*$^{-/-}$ mice. In contrast, strong matrix and pericellular type II collagen staining is apparent in DMM-operated *Panx3*$^{f/f}$:*Col2cre mice* and in sham-operated controls from each genotype (Fig. 4f). Immunostaining of MMP13, the main collagenase associated with type II collagen destruction in OA, is increased in the remaining cartilage in DMM-operated *Panx3*$^{f/f}$ mice (Fig. 4g). In contrast, DMM-operated *Panx3*$^{f/f}$:*Col2cre* and sham-operated controls of either genotype reveal minimal MMP13 staining below the calcified cartilage, but none in the articular cartilage (Fig. 4g).

Global *Panx3* Deletion Protects Against the Development of Surgically Induced OA

As our data show, cartilage-specific *Panx3* deletion protects against cartilage destruction and OA following DMM surgery. Because of the ubiquitous expression of *Panx3* in joint tissues (most notably cartilage and bone), we next examined the effects of global *Panx3* deletion on the OA development following DMM surgery. We performed DMM surgery on 20-week-old control (WT) or *Panx3*$^{-/-}$ mice. Paraffin sections of knees isolated 8 weeks

post-surgery were stained with Safranin-O/Fast Green and scored according to the OARSI histopathology scoring system. Significant joint damage was detected in DMM-operated WT control mice similar to that seen in DMM-operated *Panx3*$^{f/f}$ *mice*. In contrast, some proteoglycan loss and minimal cartilage degeneration was observed in DMM-operated *Panx3*$^{-/-}$ mice (Fig. 5a, b). Medial tibia and whole joint scores reveal statistically significant differences in the magnitude of cartilage damage seen in DMM-operated WT compared to *Panx3*$^{-/-}$ mice (Fig. 5c, e). Although there are noticeable differences in cartilage degeneration on the femoral condyles of DMM-operated WT and *Panx3*$^{-/-}$ mice, these are not significantly different (Fig. 5d).

Analysis of Osteophyte Size and Pannexin Staining in DMM-Operated *Panx3*$^{f/f}$ Mice

In addition to extensive cartilage loss, all five DMM-operated *Panx3*$^{f/f}$ mice showed extensive osteophyte formation in the medial margins of the joint. Using three slides from each animal, the average osteophyte area was calculated to be 0.138±0.0156 mm^2. No osteophytes were detected in DMM-operated *Panx3*$^{f/f}$:*Col2cre* mice or sham-operated animals of either genotype, thus prohibiting further analysis or comparisons. Immunohistochemical analysis of Panx1 and Panx3 in osteophytes revealed strong immunoreactivity in osteophytes following DMM surgery (Fig. 6a, b). Immunostaining with MMP13 antibodies revealed similar localization in these osteophytes as well (Fig. 6c). Additionally, since *Panx3*$^{fl/fl}$: *Col2cre* mice did not develop such osteophytes, it was not possible to examine whether Panx1 is upregulated in a compensatory manner. Additionally, because *Col2cre*-mediated *Panx3* deletion is not 100 % penetrant, there is low intensity Panx3 immunoreactivity throughout the cartilage of *Panx3-*$^{fl/fl}$*:Col2cre* mice. Regardless, it was apparent that Panx1 and the minimal amount of remaining Panx3 were unable to drive cartilage degeneration and OA in the surgically challenged *Panx3*$^{fl/fl}$:*Col2cre* mice.

Discussion

The pannexins are a unique three-member family of channel-forming glycoproteins. The most extensively studied and ubiquitously expressed member, Panx1, has been implicated in a diverse array of physiological and pathological processes [34–36, 15]. Recently, there has been increasing interest in elucidating the roles of Panx2 and Panx3, both of which show more restricted expression patterns [12]. Despite newer evidence suggesting a more ubiquitous expression pattern for Panx2 than previously anticipated [37], it does not appear to be expressed in bone or cartilage. Panx3, however, is expressed in prehypertrophic chondrocytes, acts to accelerate their terminal differentiation through increased ATP release [11, 17], and is upregulated in OA [10]. With the aim to further examine these roles of *Panx3 in vivo*, we generated *Panx3*$^{fl/fl}$ mice and investigated the consequence of global and cartilage-specific deletion on skeletal development and OA.

Using the *Cre/loxP* recombinase system, we targeted the second exon of *Panx3*. Exon 2 contains 143 coding nucleotides that encode ~47 amino acids corresponding to the first extracellular loop of mouse Panx3. Removal of the second exon from the gene destabilizes and ablates the expression of the entire *Panx3* mRNA and protein, as we confirmed by RT-PCR and Western blot, respectively. To our knowledge, this is the first *Panx3* null mouse

model to be reported in the literature. *Panx3*$^{-/-}$ mice were viable and fertile with no overt phenotypes to report. However, due to the less-than-Mendelian ratio of *Panx3*$^{-/-}$ offspring, we hypothesize a higher intra-uterine death rate in *Panx3*$^{-/-}$ mice. At this moment, the reason for the apparent embryonic death of KO mice is unknown.

In this study, we show that global deletion of *Panx3* does not affect gross skeletal development at P0, P21, or P42. However, because we only examined gross skeletal morphology, detailed morphometric analyses are required to determine whether subtle changes in bone morphology occur in *Panx3*$^{-/-}$ mice. Growth plate morphology is unchanged in *Panx3* null mice at P0 or P21. These findings are somewhat surprising given previous in vitro data which show that siRNA-mediated *Panx3* knock down delays hypertrophic differentiation of chondrogenic ATDC5 cells [17]. We suspect that in *Panx3*$^{-/-}$ mice, this is likely due to the ubiquitous expression of Panx1 throughout the murine growth plate in both WT and *Panx3* null long bones at P0, P21, and P42 (Supplemental Fig. 1). Panx1 and Panx3 share 59 % homology at the amino acid level, which is likely correlated to functionally similar proteins. Therefore, it is likely that these proteins have overlapping and/or redundant roles in cells co-expressing Panx1 and Panx3 such as chondrocytes [12].

However, because we see significant differences between DMM-operated control and *Panx3*-deficient mice (*Panx3*$^{-/-}$ and *Panx3*$^{f/f}$:*Col2cre*) in OA progression, there is no evidence of a compensatory effect of Panx1 in articular cartilage under these conditions. In 20-week-old mice that had undergone DMM surgery, animals lacking *Panx3* globally or specifically in cartilage showed significant protection against OA development at 8 weeks post-surgery. The substantial cartilage degeneration and joint pathology observed in DMM-operated control mice was contrasted with overall healthy joints in *Panx3*$^{f/f}$:*Col2cre* and *Panx3*$^{-/-}$ mice, which showed only minor proteoglycan loss and early degenerative changes. Our data, therefore, suggest that Panx3 is an important player in driving OA pathogenesis following joint destabilizing surgery.

Nevertheless, we do see increased Panx1 (and Panx3) staining in osteophytes, which were seen in all five DMM-operated control animals, but not *Panx3*-deficient animals (Fig. 6). Osteophytes are bony projections extending from the margins of the joint and are commonly seen in OA. A number of different factors ultimately drive their growth and development, including mechanical instability and aberrant cytokine signaling [38]. Patients presenting with these outgrowths commonly experience significant pain and joint dysfunction. Interestingly, the process driving the development and growth of these structures is highly similar to endochondral ossification, and therefore, it was not surprising that both Panx1 and Panx3 were found in abundance in these regions.

Current evidence suggests that this pathological role of Panx3 in OA could be the result of Panx3-mediated hypertrophic-like changes in articular chondrocytes in a mechanically unstable joint, possibly through ATP release. Normally, ATP is released by chondrocytes through multiple mechanisms (likely including Panx1 and Panx3) in response to physiologic mechanical stimulation [39, 40, 34, 41]. This leads to the induction of anabolic genes encoding proteins such as lubricin, aggrecan, and type II collagen, which maintain healthy cartilage and joint function [42]. In contrast, abnormal mechanical loading results in

increased ATP release, which has been linked to the induction of catabolic genes such as *Mmp13* that are critical in the pathogenesis of OA [43, 44]. Both ATP release and mechanical loading have also shown to increase levels of Runt-related transcription factor 2 (RUNX2), a potent inducer of chondrocyte hypertrophy [45, 46]. Interestingly, putative Runx2 binding sites have been identified in *Panx3* promoter sequences, indicating that Runx2 is a potential transcriptional regulator of *Panx3* expression [21].

Based on these data we hypothesize that the altered mechanical environment following joint injury leads to the Runx2-mediated induction of Panx3, enhancing ATP release from articular chondrocytes. Combined with the ATP released by other mechanisms, local extracellular ATP concentrations rise. This increase in extracellular ATP can lead to activation of purine receptors (P2Y and P2X) and downstream effectors including ERK1/2. ERK1/2, together with altered mechanical loading, further activates RUNX2 [45], leading to enhanced *Panx3* and *Mmp13* expression and cartilage matrix breakdown. This begins the vicious cycle that ultimately leads to the complete destruction of the articular cartilage and joint.

Critical to OA progression is the induction of *Mmp13 gene* expression and increased MMP13 activity. Although other pathways lead to increases in MMP13, our data suggest that increases in Panx3 are correlated with increases in MMP13. DMM surgery in 12-week-old WT mice caused mild cartilage damage 5 weeks post-surgery. Increased Panx3 immunostaining was observed in these cartilage lesions, with overlapping increases in MMP13 immunostaining. Our data also show that chondrocyte-specific *Panx3* deletion is associated with reduced MMP13 staining following DMM surgery. Furthermore, this is also associated with increased type II collagen in the articular cartilage. While loss of Panx3 potentially affects other catabolic factors as well (e.g. aggrecanases such as ADAMTS4 or 5), MMP13 is a critical catabolic enzyme in cartilage because it cleaves type II collagen, an essential structural component of the articular cartilage [47, 48]. Ultimately, genetic loss of *Panx3*, specifically in chondrocytes, protects against the development of surgically induced OA by reducing the chondrocytes ability to pathologically respond to altered mechanical loading. Equally important, loss of *Panx3* has no overt consequence on joint development and health. It is likely that Panx1 alone is sufficient to mediate relatively normal skeletal and joint development, and in permanent adult cartilage, Panx3 is not normally found in significant levels, therefore, having minimal effect on normal joint health.

In conclusion, we have successfully generated *Panx3* global and conditional mouse lines and used them to investigate the role of Panx3 in OA. This is the first study to show that genetic deletion of *Panx3* prevents the development of OA in a mouse model of joint instability-induced OA. We have thus identified Panx3, a novel channel forming glycoprotein found in human osteoarthritic tissue, as a potential target for novel OA therapies.

Supplementary Material

Refer to Web version on PubMed Central for supplementary material.

Acknowledgments

This study was funded by a Canadian Institutes of Health Research operating grant (MOP130530) to DWL, FB, and SP. DWL and FB are supported by Canada Research Chair Awards. SBA and AM are supported in part by U.S. National Institutes of Health grant R01-AR054817.

References

1. Hunter DJ, Schofield D, Callander E. The individual and socioeconomic impact of osteoarthritis. Nat Rev Rheumatol. 2014; 10(7):437–441. [PubMed: 24662640]
2. Helmick CG, Felson DT, Lawrence RC, Gabriel S, Hirsch R, Kwoh CK, Liang MH, Kremers HM, Mayes MD, Merkel PA, et al. Estimates of the prevalence of arthritis and other rheumatic conditions in the United States. Arthritis Rheum. 2008; 58(1):15–25. [PubMed: 18163481]
3. Nuesch E, Dieppe P, Reichenbach S, Williams S, Iff S, Juni P. All cause and disease specific mortality in patients with knee or hip osteoarthritis: population based cohort study. BMJ. 2011; 342:d1165. [PubMed: 21385807]
4. Lawrence RC, Felson DT, Helmick CG, Arnold LM, Choi H, Deyo RA, Gabriel S, Hirsch R, Hochberg MC, Hunder GG, et al. Estimates of the prevalence of arthritis and other rheumatic conditions in the United States. Part II Arthritis Rheum. 2008; 58(1):26–35. [PubMed: 18163497]
5. Hochberg MC, Altman RD, April KT, Benkhalti M, Guyatt G, McGowan J, Towheed T, Welch V, Wells G, Tugwell P, et al. American College of Rheumatology 2012 recommendations for the use of nonpharmacologic and pharmacologic therapies in osteoarthritis of the hand, hip, and knee. Arthritis Care Res. 2012; 64(4):465–474.
6. Weinstein AM, Rome BN, Reichmann WM, Collins JE, Burbine SA, Thornhill TS, Wright J, Katz JN, Losina E. Estimating the burden of total knee replacement in the United States. J Bone Joint Surg Am. 2013; 95(5):385–392. [PubMed: 23344005]
7. Loeser RF, Goldring SR, Scanzello CR, Goldring MB. Osteoarthritis: a disease of the joint as an organ. Arthritis Rheum. 2012; 64(6):1697–1707. [PubMed: 22392533]
8. Roach HI, Aigner T, Soder S, Haag J, Welkerling H. Pathobiology of osteoarthritis: pathomechanisms and potential therapeutic targets. Curr Drug Targets. 2007; 8(2):271–282. [PubMed: 17305505]
9. Aigner T, Sachse A, Gebhard PM, Roach HI. Osteoarthritis: pathobiology-targets and ways for therapeutic intervention. Adv Drug Deliv Rev. 2006; 58(2):128–149. [PubMed: 16616393]
10. Appleton CT, Pitelka V, Henry J, Beier F. Global analyses of gene expression in early experimental osteoarthritis. Arthritis Rheum. 2007; 56(6):1854–1868. [PubMed: 17530714]
11. James CG, Stanton LA, Agoston H, Ulici V, Underhill TM, Beier F. Genome-wide analyses of gene expression during mouse endochondral ossification. PLoS One. 2010; 5(1):e8693.10.1371/journal.pone.0008693 [PubMed: 20084171]
12. Penuela S, Gehi R, Laird DW. The biochemistry and function of pannexin channels. Biochim Biophys Acta. 2013; 1828(1):15–22. [PubMed: 22305965]
13. Panchin Y, Kelmanson I, Matz M, Lukyanov K, Usman N, Lukyanov S. A ubiquitous family of putative gap junction molecules. Curr Biol. 2000; 10(13):R473–474. [PubMed: 10898987]
14. Bennett MV, Garre JM, Orellana JA, Bukauskas FF, Nedergaard M, Saez JC. Connexin and pannexin hemichannels in inflammatory responses of glia and neurons. Brain Res. 2012; 1487:3–15. [PubMed: 22975435]
15. Penuela S, Harland L, Simek J, Laird DW. Pannexin channels and their links to human disease. Biochem J. 2014; 461(3):371–381. [PubMed: 25008946]
16. Dahl G, Keane RW. Pannexin: from discovery to bedside in 11+/−4 years? Brain Res. 2012; 1487:150–159. [PubMed: 22771709]
17. Iwamoto T, Nakamura T, Doyle A, Ishikawa M, de Vega S, Fukumoto S, Yamada Y. Pannexin 3 regulates intracellular ATP/cAMP levels and promotes chondrocyte differentiation. J Biol Chem. 2010; 285(24):18948–18958. [PubMed: 20404334]

18. van der Kraan PM, van den Berg WB. Chondrocyte hypertrophy and osteoarthritis: role in initiation and progression of cartilage degeneration? Osteoarthritis and cartilage/OARS. Osteoarthr Res Soc. 2012; 20(3):223–232.
19. Pitsillides AA, Beier F. Cartilage biology in osteoarthritis–lessons from developmental biology. Nat Rev Rheumatol. 2011; 7(11):654–663. [PubMed: 21947178]
20. D'Angelo M, Yan Z, Nooreyazdan M, Pacifici M, Sarment DS, Billings PC, Leboy PS. MMP-13 is induced during chondrocyte hypertrophy. J Cell Biochem. 2000; 77(4):678–693. [PubMed: 10771523]
21. Bond SR, Lau A, Penuela S, Sampaio AV, Underhill TM, Laird DW, Naus CC. Pannexin 3 is a novel target for Runx2, expressed by osteoblasts and mature growth plate chondrocytes. J Bone Miner Resh Off J Am Soc Bone Miner Res. 2011; 26(12):2911–2922.
22. Wang G, Woods A, Agoston H, Ulici V, Glogauer M, Beier F. Genetic ablation of Rac1 in cartilage results in chondrodysplasia. Dev Biol. 2007; 306(2):612–623. [PubMed: 17467682]
23. Solomon LA, Li JR, Berube NG, Beier F. Loss of ATRX in chondrocytes has minimal effects on skeletal development. PLoS One. 2009; 4(9):e7106.10.1371/journal.pone.0007106 [PubMed: 19774083]
24. Gillespie JR, Ulici V, Dupuis H, Higgs A, Dimattia A, Patel S, Woodgett JR, Beier F. Deletion of glycogen synthase kinase-3beta in cartilage results in up-regulation of glycogen synthase kinase-3alpha protein expression. Endocrinology. 2011; 152(5):1755–1766. [PubMed: 21325041]
25. Pest MA, Russell BA, Zhang YW, Jeong JW, Beier F. Disturbed cartilage and joint homeostasis resulting from a loss of mitogen-inducible gene 6 in a mouse model of joint dysfunction. Arthritis Rheumatol. 2014; 66(10):2816–2827. [PubMed: 24966136]
26. Penuela S, Bhalla R, Nag K, Laird DW. Glycosylation regulates pannexin intermixing and cellular localization. Mol Biol Cell. 2009; 20(20):4313–4323. [PubMed: 19692571]
27. Penuela S, Bhalla R, Gong XQ, Cowan KN, Celetti SJ, Cowan BJ, Bai D, Shao Q, Laird DW. Pannexin 1 and pannexin 3 are glycoproteins that exhibit many distinct characteristics from the connexin family of gap junction proteins. J Cell Sci. 2007; 120(Pt 21):3772–3783. [PubMed: 17925379]
28. Glasson SS, Blanchet TJ, Morris EA. The surgical destabilization of the medial meniscus (DMM) model of osteoarthritis in the 129/SvEv mouse. Osteoarthr Cartil/OARS Osteoarthr Res Soc. 2007; 15(9):1061–1069.
29. Welch ID, Cowan MF, Beier F, Underhill TM. The retinoic acid binding protein CRABP2 is increased in murine models of degenerative joint disease. Arthritis Res Ther. 2009; 11(1):R14. [PubMed: 19173746]
30. Ratneswaran A, LeBlanc EA, Walser E, Welch I, Mort JS, Borradaile N, Beier F. Peroxisome proliferator-activated receptor delta promotes the progression of posttraumatic osteoarthritis in a mouse model. Arthritis Rheum. 2015; 67(2):454–464.
31. Usmani SE, Pest MA, Kim G, Ohora SN, Qin L, Beier F. Transforming growth factor alpha controls the transition from hypertrophic cartilage to bone during endochondral bone growth. Bone. 2012; 51(1):131–141. [PubMed: 22575362]
32. Glasson SS, Chambers MG, Van Den Berg WB, Little CB. The OARSI histopathology initiative - recommendations for histological assessments of osteoarthritis in the mouse. Osteoarthr Cartil/OARS Osteoarthr Res Soc. 2010; 18(Suppl 3):S17–23.
33. Schwenk F, Baron U, Rajewsky K. A cre-transgenic mouse strain for the ubiquitous deletion of loxP-flanked gene segments including deletion in germ cells. Nucleic Acids Res. 1995; 23(24): 5080–5081. [PubMed: 8559668]
34. Chekeni FB, Elliott MR, Sandilos JK, Walk SF, Kinchen JM, Lazarowski ER, Armstrong AJ, Penuela S, Laird DW, Salvesen GS, et al. Pannexin 1 channels mediate 'find-me' signal release and membrane permeability during apoptosis. Nature. 2010; 467(7317):863–867. [PubMed: 20944749]
35. Billaud M, Sandilos JK, Isakson BE. Pannexin 1 in the regulation of vascular tone. Trends Cardiovasc Med. 2012; 22(3):68–72. [PubMed: 22841835]

36. Poon IK, Chiu YH, Armstrong AJ, Kinchen JM, Juncadella IJ, Bayliss DA, Ravichandran KS. Unexpected link between an antibiotic, pannexin channels and apoptosis. Nature. 2014; 507(7492):329–334. [PubMed: 24646995]

37. Le Vasseur M, Lelowski J, Bechberger JF, Sin WC, Naus CC. Pannexin 2 protein expression is not restricted to the CNS. Front Cell Neurosci. 2014; 8:392. [PubMed: 25505382]

38. van der Kraan PM, van den Berg WB. Osteophytes: relevance and biology. Osteoarthr Cartil. 2007; 15(3):237–244. [PubMed: 17204437]

39. Garcia M, Knight MM. Cyclic loading opens hemichannels to release ATP as part of a chondrocyte mechanotransduction pathway. J Orthop Res Off Pub Orthop Res Soc. 2010; 28(4): 510–515.

40. Graff RD, Lazarowski ER, Banes AJ, Lee GM. ATP release by mechanically loaded porcine chondrons in pellet culture. Arthritis Rheum. 2000; 43(7):1571–1579. [PubMed: 10902762]

41. Ishikawa M, Iwamoto T, Nakamura T, Doyle A, Fukumoto S, Yamada Y. Pannexin 3 functions as an ER Ca(2+) channel, hemichannel, and gap junction to promote osteoblast differentiation. J Cell Biol. 2011; 193(7):1257–1274. [PubMed: 21690309]

42. Ogawa H, Kozhemyakina E, Hung HH, Grodzinsky AJ, Lassar AB. Mechanical motion promotes expression of Prg4 in articular cartilage via multiple CREB-dependent, fluid flow shear stress-induced signaling pathways. Genes Dev. 2014; 28(2):127–139. [PubMed: 24449269]

43. Waldman SD, Usprech J, Flynn LE, Khan AA. Harnessing the purinergic receptor pathway to develop functional engineered cartilage constructs. Osteoarthr Cartil/OARS Osteoarthr Res Soc. 2010; 18(6):864–872.

44. Leong WS, Russell RG, Caswell AM. Stimulation of cartilage resorption by extracellular ATP acting at P2-purinoceptors. Biochim Biophys Acta. 1994; 1201(2):298–304. [PubMed: 7947945]

45. Papachristou DJ, Pirttiniemi P, Kantomaa T, Papavassiliou AG, Basdra EK. JNK/ERK-AP-1/Runx2 induction “paves the way” to cartilage load-ignited chondroblastic differentiation. Histochem Cell Biol. 2005; 124(3–4):215–223. [PubMed: 16041628]

46. Costessi A, Pines A, D’Andrea P, Romanello M, Damante G, Cesaratto L, Quadrifoglio F, Moro L, Tell G. Extracellular nucleotides activate Runx2 in the osteoblast-like HOBIT cell line: a possible molecular link between mechanical stress and osteoblasts’ response. Bone. 2005; 36(3):418–432. [PubMed: 15777650]

47. Billinghurst RC, Dahlberg L, Ionescu M, Reiner A, Bourne R, Rorabeck C, Mitchell P, Hambor J, Diekmann O, Tschesche H, et al. Enhanced cleavage of type II collagen by collagenases in osteoarthritic articular cartilage. J Clin Invest. 1997; 99(7):1534–1545. [PubMed: 9119997]

48. Knauper V, Lopez-Otin C, Smith B, Knight G, Murphy G. Biochemical characterization of human collagenase-3. J Biol Chem. 1996; 271(3):1544–1550. [PubMed: 8576151]

Key message

- Panx3 is localized to cartilage lesions in mice and humans.
- Global *Panx3* deletion does not result in any developmental abnormalities.
- Mice lacking *Panx3* are resistant to the development of osteoarthritis.
- Panx3 is a novel therapeutic target for the treatment of osteoarthritis.

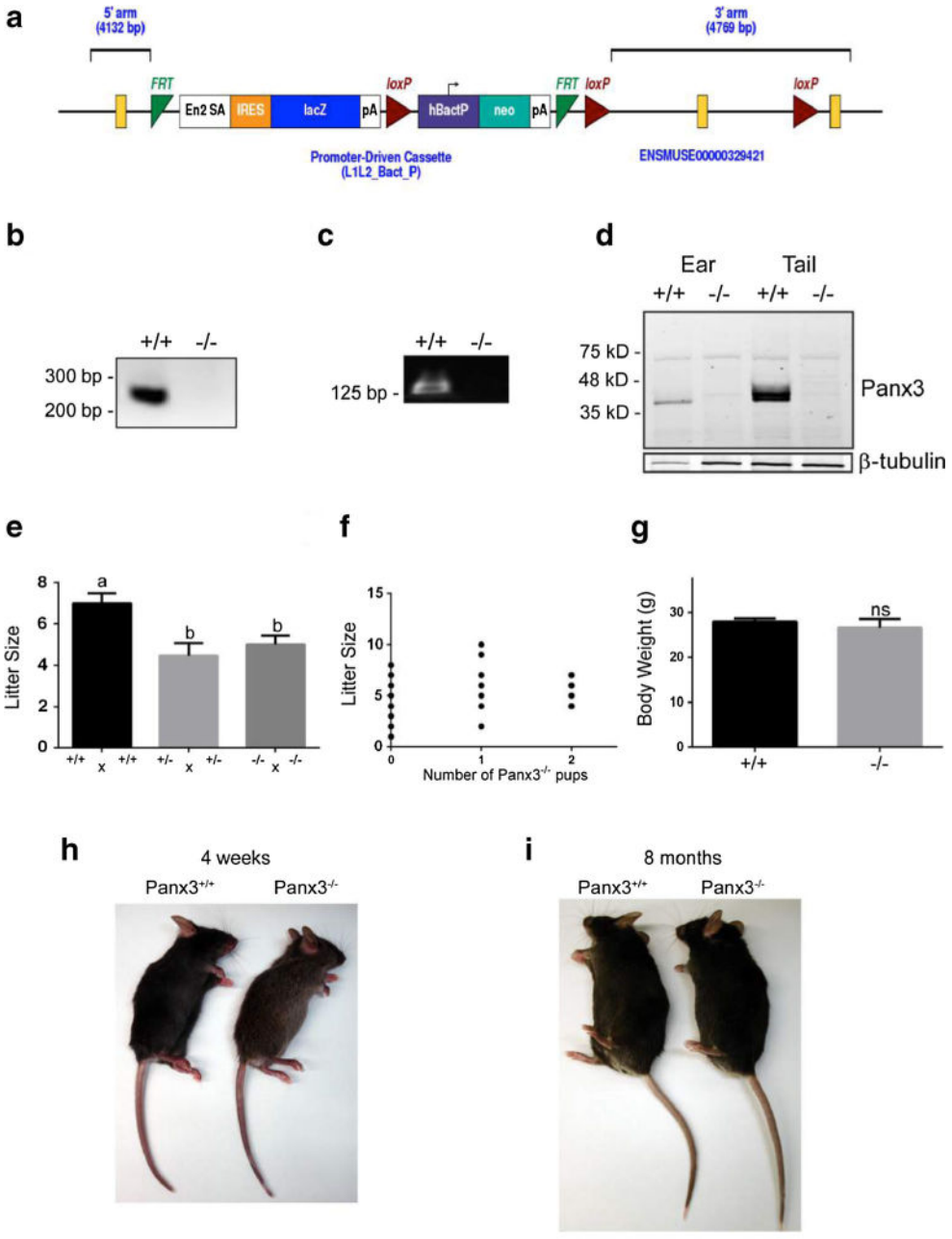

Fig. 1.

Generation of *Panx3*$^{-/-}$ mice. **a** *Panx3* targeting vector from KOMP project ID CSD24494. The "Knockout-First" reporter tagged insertion promoter-driven cassette targets the second exon of *Panx3*, creating a truncated protein product. Source: www.knockoutmouse.org. **b** PCR genotyping showing lack of Panx3 exon2 amplicon in Panx3 null mice (Panx3$^{-/-}$). Upper primer is in the intron upstream of exon 2 in the floxed allele; the lower primer is in exon 2. PCR produces a 232-bp in the wild type (Panx3$^{+/+}$), but not in the null. **c** RT-PCR of mRNA from the mouse cartilage, using primers designed to amplify a 128-bp product bridging the intron between exons 3 and 4 of Panx3, revealed no amplification in the null mouse. **d** Western blots of protein lysates from wild type and Panx3$^{-/-}$ mouse cartilage

confirmed the complete absence of Panx3 protein in the $Panx3^{-/-}$ mice. β-tubulin was used as loading control. **e** Litter size was significantly reduced in $Panx3^{+/-} \times Panx3^{+/-}$ crosses as well as $Panx3^{-/-} \times Panx3^{-/-}$ crosses compared to $Panx3^{+/+} \times Panx3^{+/+}$ crosses (N=13 litters, P<0.05; one-way ANOVA followed by Tukey test). weight of a 3-month-old $Panx3^{-/-}$ male mice was not significantly different (ns) to $Panx3^{+/+}$ controls (N=10, t test, P>0.05). A 4-week-old (**h**) and an 8-month-old males examined (i) showed no overt morphological phenotypes when compared to $Panx3^{+/+}$ controls.

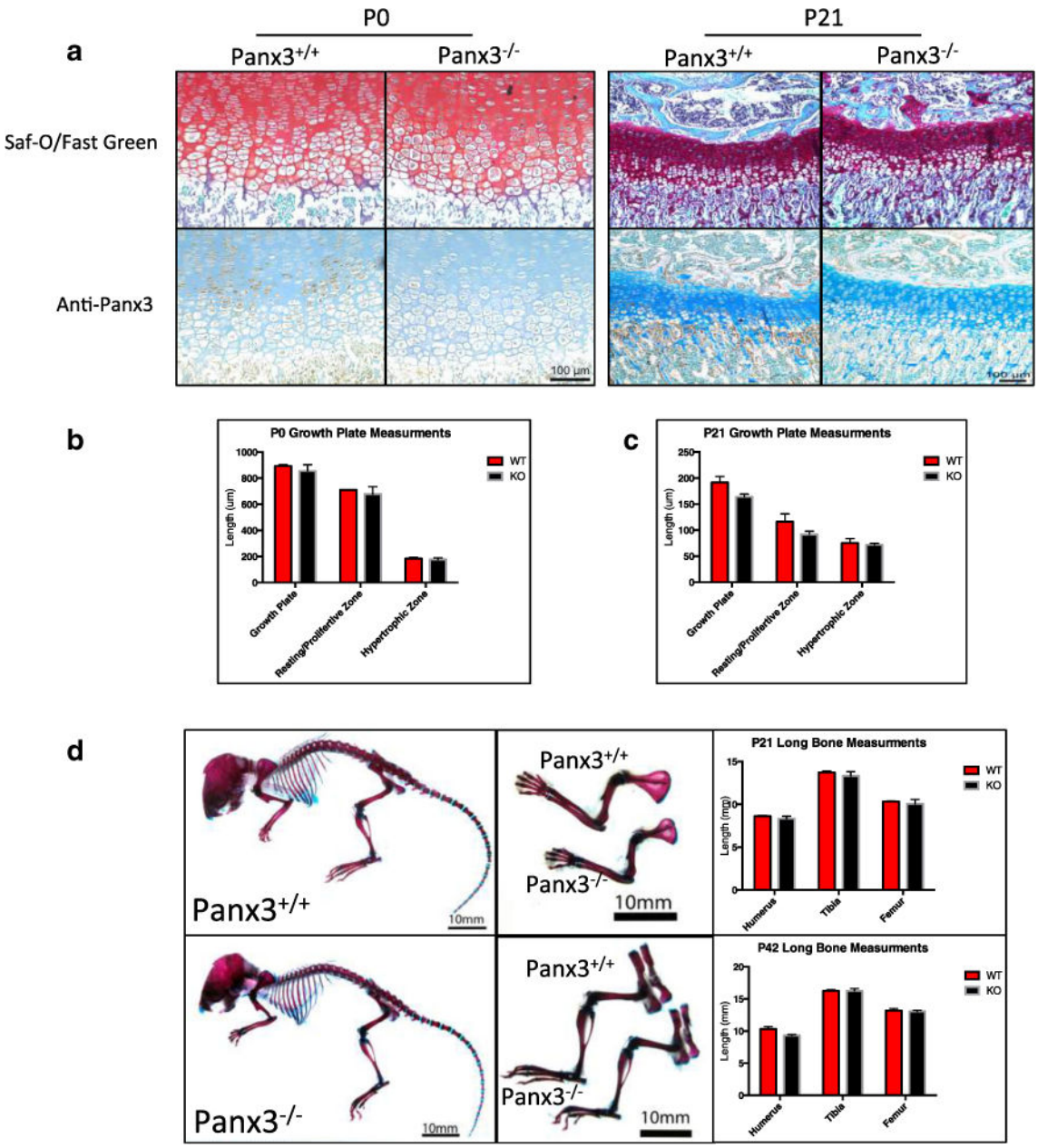

Fig. 2.

Global loss of *Panx3* has no effect on the development of the murine skeleton. Newborn (P0), 21 day old (P21), and 42 day old (P42) wild-type (WT) and *Panx3* null mice were examined for signs of abnormal skeletal development. **a** Representative images of Safranin-O/Fast Green stained sections of WT and *Panx3*$^{-/-}$ tibia growth plates at P0 and P21. **b**, **c** Measurements of total growth plate, resting/proliferative zone, and hypertrophic zone length at P0 and P21, respectively, show no significant size differences (N=3 WT-null pairs, P<0.05; two-tailed t test). **d** Photographs of Alizarin Red/Alcian Blue-stained whole skeletons (*left*) and upper (*top middle*) and lower (*bottom middle*) limbs of 21-day-old mice. Long bone measurements of P21 (*top right*) and P42 (*bottom right*) long bones show no size

differences between WT and *Panx3* null mice (*N*=3 WT-null pairs for each time point, $P<0.05$; two-tailed *t* test). Results show mean ± SEM.

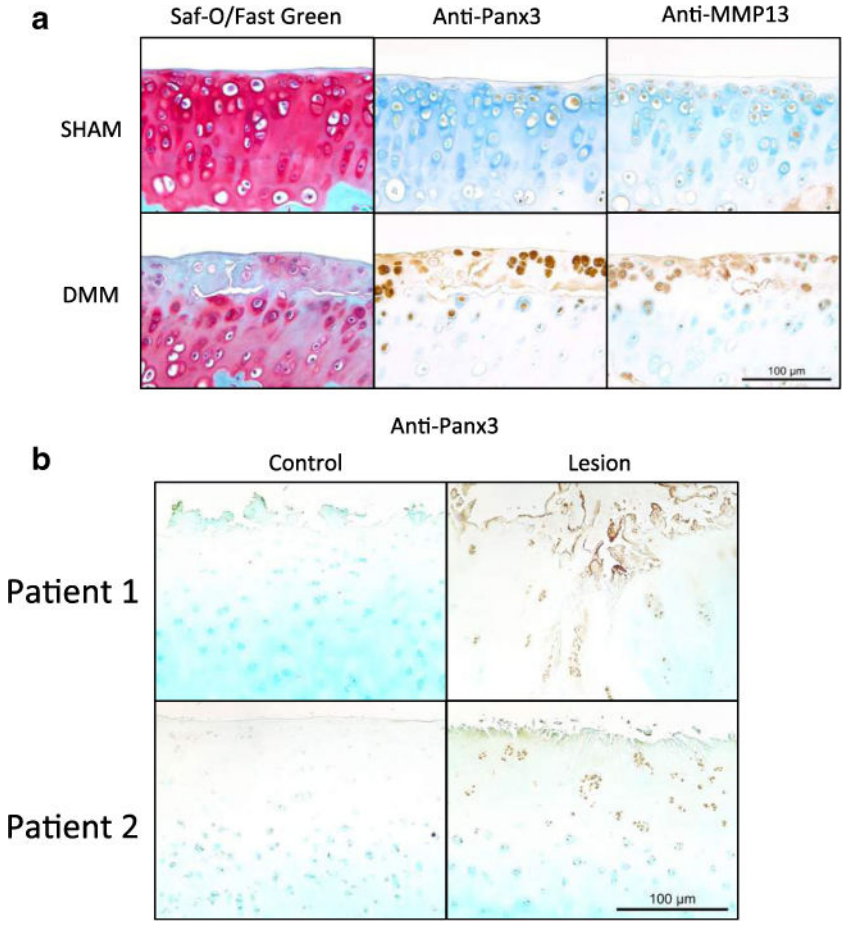

Fig. 3.

Panx3 and MMP13 are seen in chondrocyte clusters in early cartilage lesions after DMM surgery in mice and in human osteoarthritic cartilage. **a** Sham and DMM operated joints were stained with Safranin-O/Fast Green (*left*). Serial sections were immunostained using anti-Panx3 (*middle*) and anti-MMP13 (*right*) antibodies. **b** Cartilage isolated from lesioned and non-lesioned areas of human knee joints were immunostained for Panx3.

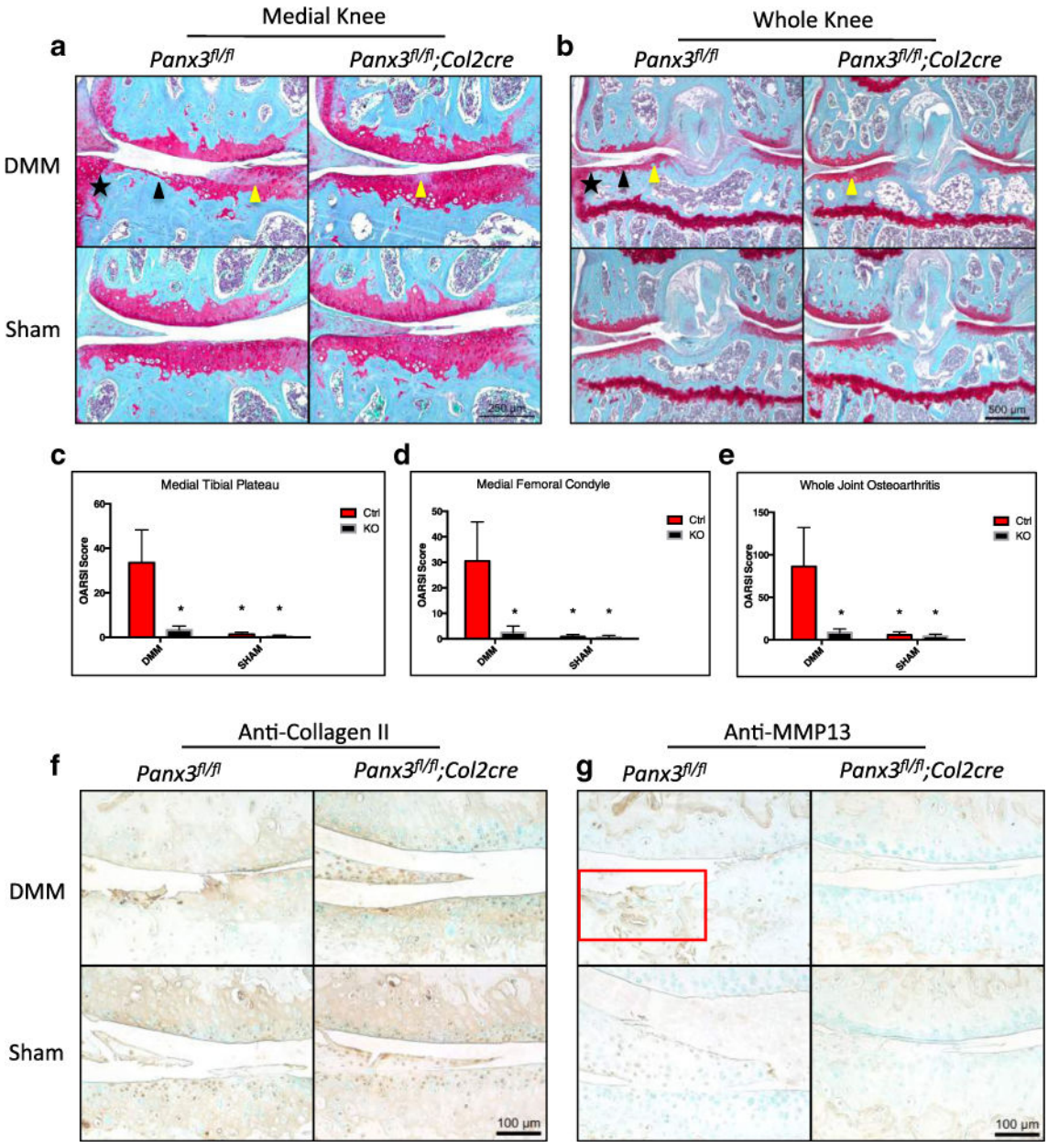

Fig. 4.

Chondrocyte specific loss of *Panx3* protects against the development of surgically induced OA in mice. Representative images of Safranin-O/Fast Green-stained sections of *Panx3*$^{fl/fl}$ and *Panx3*$^{fl/fl}$; *Col2cre*$^{+/-}$ DMM and Sham operated knees 8 weeks post-surgery (**a**, **b**). *Black arrows* indicate cartilage erosion. *Yellow arrows* indicate proteoglycan loss. *Black stars* indicate osteophyte formation. Medial knee and whole joint images were acquired. Cumulative OARSI scores of the medial tibia plateau (**c**), medial femoral condyle (**d**), and entire joint (**e**) are shown. *Asterisk* indicate means significantly different from Ctrl DMM scores (N=5, 4 DMM, sham per genotype; P<0.05, two-way ANOVA followed by Tukey's test. Expressed as mean ± SEM. Serial sections from sham and DMM-operated joints harvested from *Panx3*$^{f/f}$ and *Panx3*$^{f/f}$:*Col2cre* mice were immunostained with anti-collagen

II and anti-MMP13 antibodies (**f**, **g**). Counter staining was done using methyl green. The *red box* highlights increased MMP13 immunolabeling within degenerated cartilage.

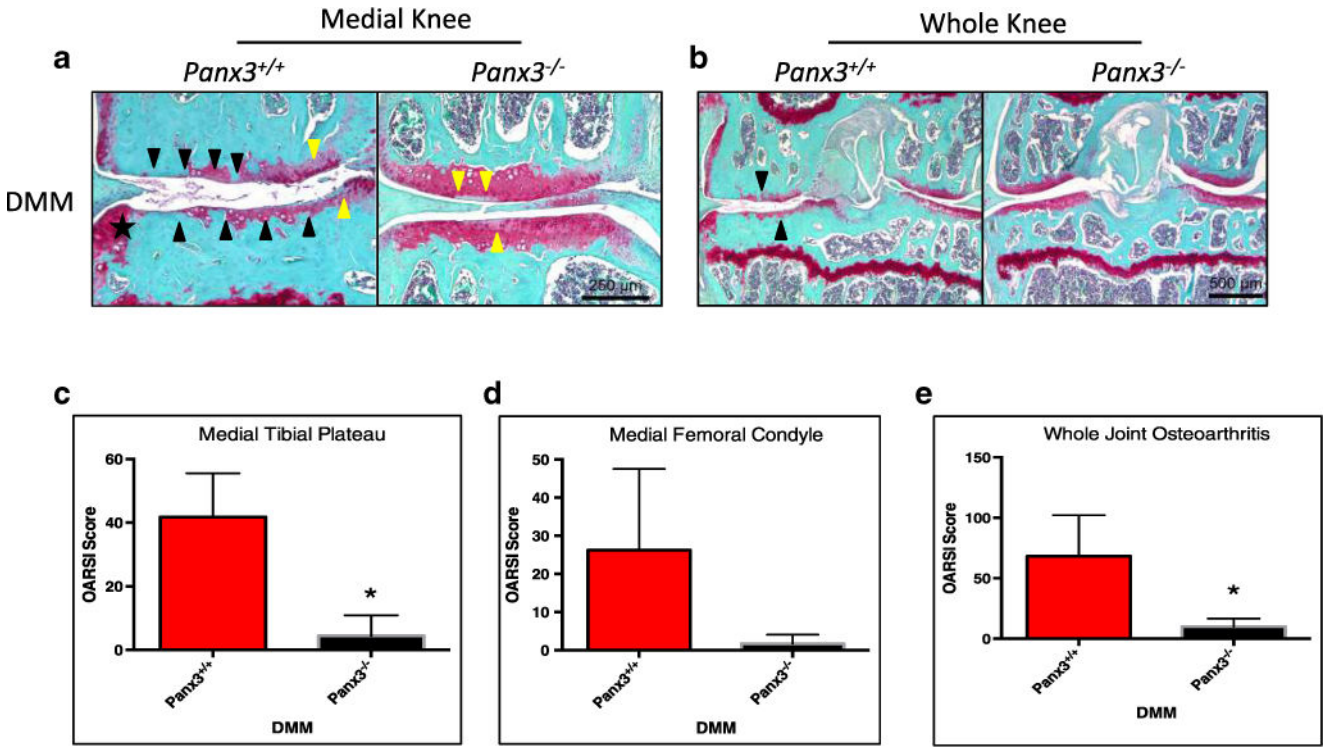

Fig. 5.

Global loss of *Panx3* protects against the development of surgically induced OA. Representative images of Safranin-O/Fast Green stained sections of WT and *Panx3*$^{-/-}$ DMM-operated knees 8 weeks post-surgery (**a**, **b**). *Black arrows* indicate cartilage erosion, while *yellow arrows* denote proteoglycan loss. The *black star* indicates the location of an osteophyte. Cumulative OARSI scores of the medial tibia plateau (**c**), medial femoral condyle (**d**), and entire joint (**e**) are shown. *Asterisk* indicates significantly different from WT DMM scores (N=3, P<0.05; two-tailed t test). Expressed as mean ± SEM.

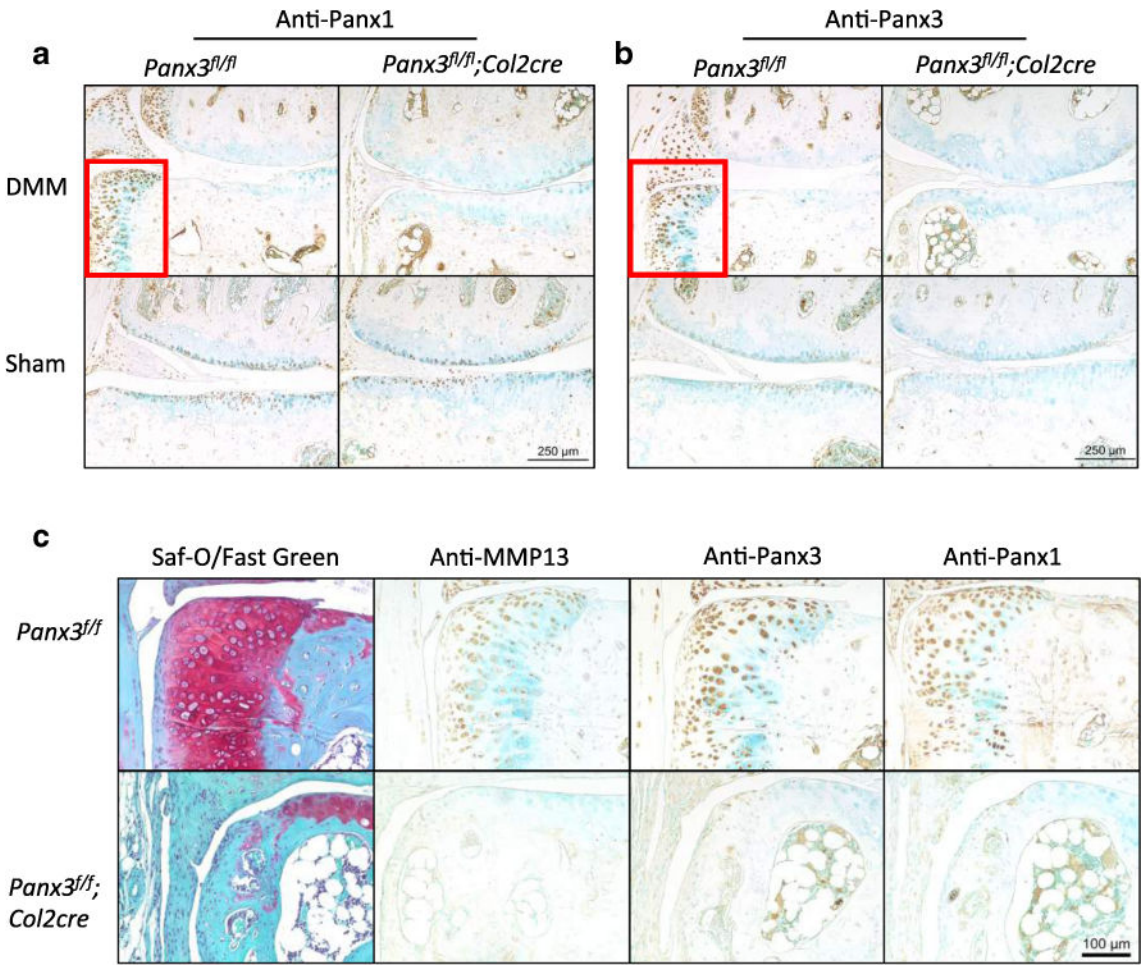

Fig. 6.

Extensive osteophyte formation is detected in all DMM operated *Panx3*$^{f/f/}$ mice and is associated with increased MMP13, Panx1, and Panx3 staining. Serial sections from DMM-operated joints harvested from *Panx3*$^{fl/f}$ and *Panx3*$^{fl/fl}$:*Col2cre* mice were immunostained with anti-Panx1 (**a**, **c**), anti-Panx3 (**b**, **c**), or anti-MMP13 (**c**) antibodies. Counterstaining was done using methyl green. Osteophyte formation was only detected in *Panx3*$^{fl/f}$ DMM-operated knees.